

OEIC-Enabling LCI Lasers with Current Guides: Combined Theoretical–Experimental Investigation of Internal Operating Mechanisms

Edward H. Sargent, *Student Member, IEEE*, Kunishige Oe, *Member, IEEE*, Catherine Caneau, and J. M. Xu, *Senior Member, IEEE*

Abstract—Lateral current injection (LCI) lasers are promising candidates for optoelectronic integration and novel functional devices. We investigate experimentally the performance of a new class of LCI lasers with improved operating characteristics, focusing in particular on regions of agreement and disagreement with our physical model. We then employ fully self-consistent two-dimensional modeling in order to study the impact on performance of current guides—vertical structures intended to lower the series resistance of the active region—and find that these structures were central to achieving improved performance. We find that with additional refinements in the design of LCI lasers with current guides, further improvements in CW room-temperature performance may be achieved.

Index Terms—Integrated optoelectronics, optoelectronic devices, semiconductor device fabrication, semiconductor device modeling, semiconductor heterojunctions, semiconductor lasers.

I. INTRODUCTION

LATERAL current injection (LCI) lasers have long been recognized to be promising candidates for use as active sources in optoelectronic integrated circuits and as functional devices. While growth on semi-insulating material allows effective interdevice isolation, there are more general advantages: LCI lasers take advantage of the lateral degree of freedom, a dimension much less richly explored than the vertical and longitudinal directions. By exploiting the lateral direction, LCI lasers may enable new functional optoelectronic devices: for example, multiple-terminal lasers with high-speed capacitive modulation and wavelength tuning [1] become possible through the use of little or no doping in the vertical heterostructure. New freedoms are also gained in the design of simple two-terminal laser structures, allowing electrical and optical designs to be partially or completely decoupled, permitting independent optimization of optical confinement and electrical injection.

In spite of this potential, LCI lasers have, until recently, exhibited performance inferior to that of their vertical injection

counterparts. Though the lateral injection concept is nearly as old as the semiconductor laser itself, LCI lasers have not benefitted from the countless iterations of theoretical study, design and process optimization, and experimental probing that vertical injection lasers have enjoyed. As a result, many of the predominantly empirical attempts at realizing LCI lasers [2]–[9] yielded devices with high threshold currents, low initial efficiency, and rapid roll-off in efficiency even at low optical powers.

Oe *et al.* [10] recently reported a novel LCI laser with much more competitive performance. Using a simple bulk active region, they obtained a device which lased at 1.55 μm CW and at room temperature with a threshold of 10 mA and optical powers per facet in excess of 10 mW. The basic structure of this device, whose fabrication is reported in detail in [10], is illustrated in the inset of Fig. 1. Current guides—doped layers of intermediate composition—are placed above and below the active region. The current guides were shown using two-dimensional (2-D) fully self-consistent numerical simulation to smooth out the lateral material gain profile in the device [11], permitting efficient pumping of the fundamental optical mode. It has been shown [12] that conventional LCI lasers which do not employ current guides typically suffer from inefficient pumping of the fundamental optical mode because their lateral carrier density distribution may be highly nonuniform. This inefficiency may be severe if the contacts are separated by more than the ambipolar diffusion length of carriers, a quantity which in turn is limited by the low mobility of heavy holes in compound semiconductors. Current guides achieve improved gain uniformity by using hybrid injection of carriers [11], a combination of lateral and vertical injection.

Another effect of current guides is to reduce the series resistance of the active region by increasing the area available for the injection of a given current. Resistive heating is decreased as a result, making CW room-temperature operation feasible. In addition, as voltage accumulates more slowly across leakage paths in parallel with the active region, the onset of significant leakage current occurs at higher optical powers.

In this paper, we assess using a combination of experiment and simulation the importance of the improvements offered by current guides. We begin by exploring the detailed temperature evolution of the measured threshold current and threshold voltage of a particular LCI laser with current guides. We

Manuscript received January 9, 1998; revised March 31, 1998.

E. H. Sargent and J. M. Xu are with the Department of Electrical and Computer Engineering, University of Toronto, Toronto, ON, M5S 1A4, Canada.

K. Oe is with NTT Opto-electronics Laboratories, Kanagawa, 243-01 Japan.

C. Caneau was with Bellcore, Red Bank, NJ 07701 USA. She is now with Corning Inc., Red Bank, NJ 07701 USA.

Publisher Item Identifier S 0018-9197(98)04568-0.

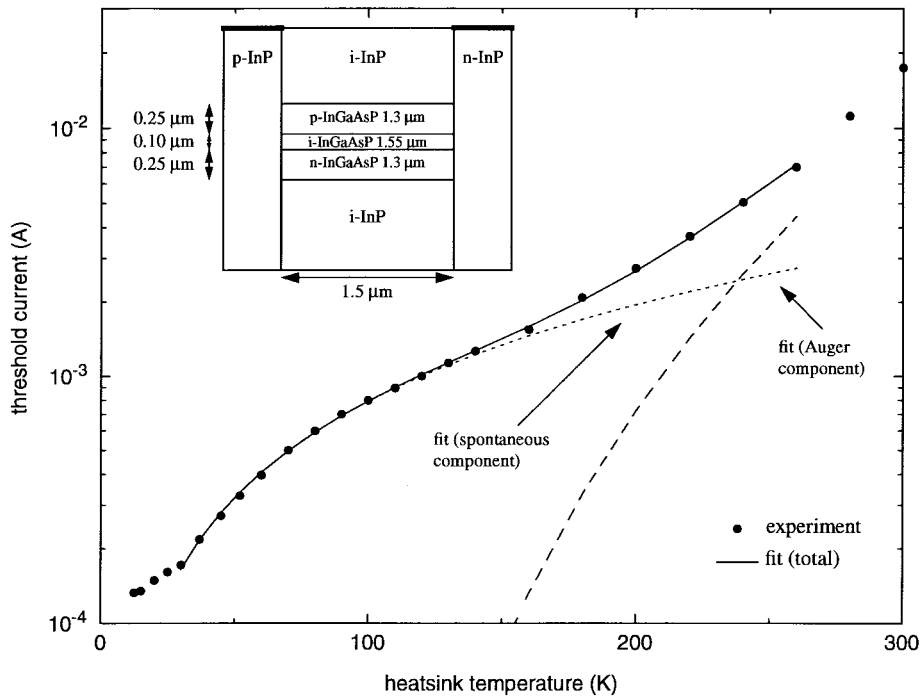


Fig. 1. Experiment: measured threshold current as a function of heatsink temperature, along with curve fit based on a simple physical model incorporating spontaneous and Auger recombination.

examine the different regions of operation of this device, focusing on temperature ranges in which different physical mechanisms dominate the performance of the device. We then proceed to study the internal operating mechanisms of a variety of LCI lasers using physical modeling. We conclude with a discussion of new qualitative and quantitative rules to guide the design of LCI lasers with improved high-power performance.

II. EXPERIMENT

We studied experimentally the LCI laser illustrated in Fig. 1 whose fabrication is reported in greater detail elsewhere [10]. The epitaxial structure consisted of a $0.1\text{-}\mu\text{m}$ -thick undoped bulk active region ($\lambda = 1.55\ \mu\text{m}$) clad above and below by $0.25\text{-}\mu\text{m}$ -thick n- and p-doped current guides ($\lambda = 1.3\ \mu\text{m}$) and undoped InP. P-type and n-type lateral contacts were formed by dry etching followed by liquid phase epitaxial overgrowth. While the device reported in [10] had a $1\text{-}\mu\text{m}$ -wide active region, in this paper we focus on a device with a wider active region. While it exhibited worse performance, this $1.5\text{-}\mu\text{m}$ -wide device was expected to be more revealing of the effects of series resistance and lateral carrier density nonuniformity.

We characterized this device over temperatures ranging from 10 to 300 K. We plot in Fig. 1 the evolution of threshold current with temperature. We derived a simple analytical expression from which to predict the temperature dependence of the threshold current, assuming: 1) that leakage effects were negligible at threshold; 2) that the bulk active region threshold carrier density obeyed an approximate $T^{3/2}$ temperature dependence; 3) that the bimolecular coefficient B obeyed a $T^{-3/2}$ dependence; and 4) that the Auger coefficient C obeyed an exponential characteristic with activation energy 53

meV. Assumption 1) is consistent with the results of physical modeling reported later in this work. Assumptions 2) and 3) are obtained from the relationships between the quasi-Fermi levels, carrier densities, and spontaneous and stimulated transition rates in bulk material. Assumption 4) is predicted theoretically and observed empirically in [13]. As shown in Fig. 1, we obtained excellent agreement between this simple model and experimentally measured threshold currents over the temperature range 30–260 K. Based on the resulting fitting parameters, we estimated the room-temperature bimolecular coefficient and Auger coefficient to be $B = 2 \times 10^{-10}\ \text{cm}^3 \cdot \text{s}^{-1}$ and $C = 5 \times 10^{-28}\ \text{cm}^6 \cdot \text{s}^{-1}$.

The experimental results and fit agree well in the temperature range 30–260 K. At very low temperatures, the temperature dependence of the threshold current levels out rather than continuing the more rapid decrease predicted from simple spontaneous emission/gain considerations. We investigated this effect further by studying the dependence of threshold voltage on temperature (Fig. 2). Even though the threshold current continues to decrease with temperature, the threshold voltage shows a sudden upward turn as the temperature is decreased below 25 K. While the bandgap of the active region is expected to increase with decreasing temperature, it is expected to do so [14] in the more gradual fashion seen between 50 and 150 K in Fig. 2. A more likely explanation relates to mobility of holes in InP, which can exhibit a sudden decrease below about 30 K with the onset of impurity conduction [15]. This would suggest a sudden and rapid decrease in ambipolar diffusion length below this critical temperature. We suggest that this mechanism, and the resulting reduced overlap of gain and fundamental optical mode, is responsible for the reduced rate of decrease in threshold with decreasing temperature at sub-30 K temperatures.

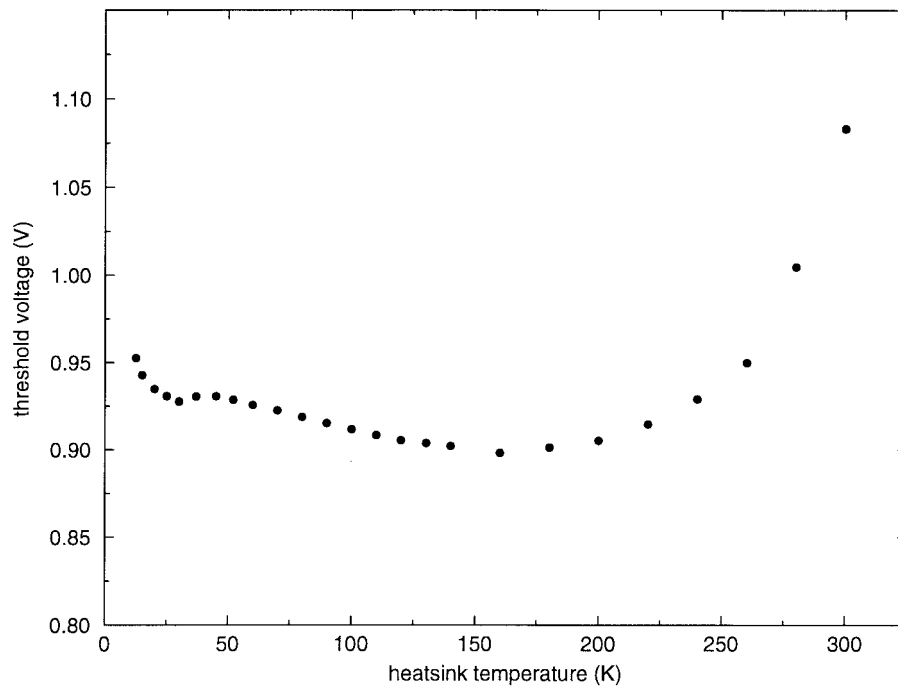


Fig. 2. Experiment: dependence of threshold voltage on heatsink temperature in the LCI laser with 1.5- μm -wide active region.

The I_{th} versus T characteristic deviates above the prediction of our simple model above 260 K. A number of mechanisms could give rise to such a qualitative dependence—we describe these first and then proceed to discuss which is most important quantitatively. First, the hole mobility decreases with increasing temperature as of ~ 50 K up to and above room temperature (as polar optical phonon scattering limits the mobility), so that the ambipolar diffusion length also decreases with increasing temperature in this range, giving rise to a more nonuniform lateral carrier density. Second, the threshold voltage of 1.1 V at 300 K is approaching a range in which leakage through the high bandgap cladding regions above and below the active regions may contribute to an increased threshold current. This concept and its consequences are the focus of Section III. Finally, measurements were made in CW mode, and the current-excess voltage product is sufficiently high at room temperature for nonnegligible Joule heating to increase the steady-state temperature of the device active region.

By comparing pulsed-mode and CW threshold currents, we confirmed heating effects to be the dominant cause of the threshold current exceeding the prediction of the simple model near room temperature. This is consistent with the results reported below in which lateral carrier density nonuniformity and parallel leakage are not found to be quantitatively important at room-temperature threshold.

III. PHYSICAL MODELING

We now consider in detail the physical mechanisms which underlie the measured performance of this new family of LCI lasers with current guides. We consider first the effect of current guiding layers on the lateral gain profile. It was previously demonstrated [11] that current guiding layers can smooth out the lateral gain profile, even in a device whose

lateral contact separation exceeds the ambipolar diffusion length of carriers, by permitting hybrid (lateral and vertical) injection of carriers into the active region. In particular, holes, which represent the lower mobility and therefore the limiting carrier in most compound semiconductor materials, benefit from having additional injection paths available for transport into the active region.

In order to assess the impact of the use of current guides, we modeled, using our fully self-consistent 2-D light-emitter simulator [16], a number of structures with and without current guides. Material parameters used are given in Table I. We have not introduced phenomenological factors such as “scattering loss” or “intrinsic loss” or higher Auger recombination coefficients. While our quantitative predictions are therefore not in exact agreement with measured results, it is shown below that our qualitative conclusions are of an interest and importance which is independent of their exact magnitude or point of onset.

We first considered the three structures illustrated in Fig. 3. One incorporates current guides similar to those employed by Oe *et al.* [10], one uses no current guides, and the final extreme case uses not only current guides but also employs doped cladding material for additional hybrid injection and further reduced series resistance. In spite of the differences in the vertical heterostructures of these devices, we imposed for the purposes of simulation identical refractive index profiles. The mode profiles were therefore identical, allowing us to assess the impact of current guiding without needing to adjust for differences in confinement factors.

The L - I and V - L characteristics of these three devices are shown in Fig. 4. (A V - L characteristic was produced instead of a V - I characteristic, the optical power L being a better measure of the current injected into the active region.) The

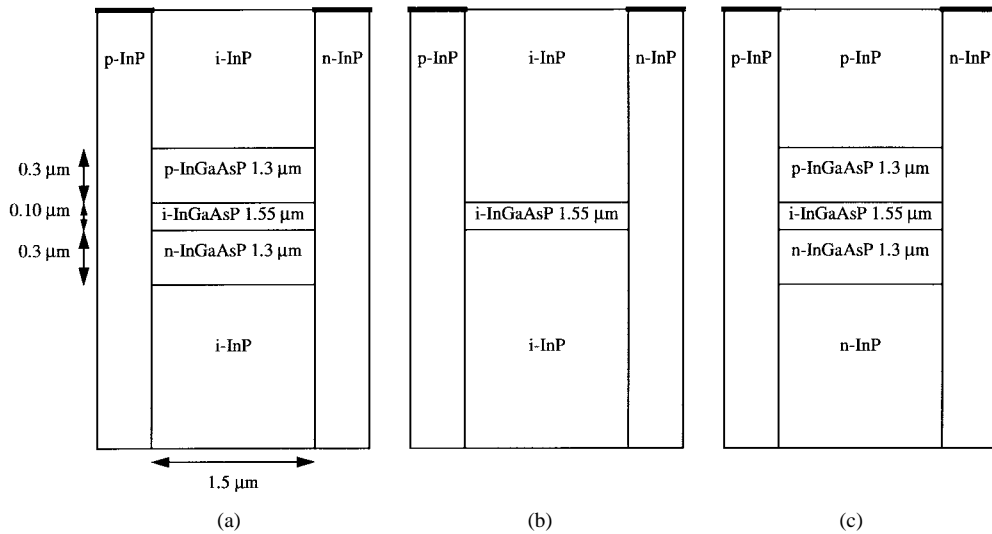


Fig. 3. Structures simulated to reveal the impact of current guides and associated hybrid injection. While not indicated explicitly in the figure, the three structures contained identical vertical refractive index profiles in order to achieve the same modal profiles and confinement factors, enabling thereby fair comparison of device performance: (a) 0.3- μm -thick current guides, (b) no current guides, and (c) doped current guides and cladding.

TABLE I
MATERIAL PARAMETERS

Quantity	Value
Electron intraband absorption	$\alpha_{\text{electron}} = (3 \times 10^{-18} \text{ cm}^2) \times n$
Hole intraband absorption	$\alpha_{\text{hole}} = (7 \times 10^{-18} \text{ cm}^2) \times p$
Material gain	$g(n) = 2.5 \times 10^{-16} \text{ cm}^2 \times (n - 8 \times 10^{17} \text{ cm}^{-3})$
Electron mobility	$3500 \text{ cm}^2/\text{Vs}$
Hole Mobility	$200 \text{ cm}^2/\text{Vs}$
n-type background doping	$1 \times 10^{15} \text{ cm}^{-3}$
P-contact doping	$2 \times 10^{18} \text{ cm}^{-3}$ except where otherwise noted
N-contact doping	$2 \times 10^{18} \text{ cm}^{-3}$ except where otherwise noted
Shockley-Read-Hall Recombination time	10 ns
Spontaneous recombination rate	$R_{\text{spont}} = (0.9 \times 10^{-10} \text{ cm}^3 \text{ s}^{-1}) np$
Auger recombination rate	$R_{\text{spont}} = (2.95 \times 10^{-29} \text{ cm}^6 \text{ s}^{-1}) \left(\frac{n^2 p + n p^2}{2} \right)$

L - I characteristics in Fig. 4(a) show a pronounced roll-off in lasing efficiency in the case of the device without current guides, while the deterioration comes much later in the case of the devices with current guides. Because it had less doping near the active region, the device without current guides experienced lower free-carrier absorption induced optical loss and exhibited therefore a slightly lower threshold current and higher initial efficiency. This advantage was soon more than offset by the disadvantage of faster roll-off in efficiency.

We posited two potentially important factors contributing to the faster roll-off of the device without current guides. First, current guides were expected [10] and shown [11] to

smooth out the lateral carrier density and gain distributions by enabling hybrid injection of carriers. We show in Fig. 5 the calculated lateral carrier density distribution for the three devices considered at different injection levels. As predicted, hybrid injection aids in smoothing out the lateral gain profile.

There remains the question of the *importance* of a more uniform lateral carrier density. Qualitatively, there are a number of mechanisms at work. Since the optical mode distribution is laterally symmetric and the carrier density distribution is not, the overlap of these distributions is weaker, and the optical mode is less efficiently pumped. As the nonuniformity increases with increasing optical power, the overlap decreases further, and a larger average carrier density must be supplied in order to satisfy the round-trip gain condition. Furthermore, a nonuniform carrier density distribution suffers more from recombination mechanisms which have superlinear carrier density dependencies. Thus, carrier density nonpinning above the lasing threshold contributes to an increased parasitic recombination current due to bimolecular and Auger mechanisms.

To assess the importance of these effects, each one linked to the lateral carrier density nonuniformity, we plot in Fig. 6 the evolution of various current components as a function of stimulated optical power per facet. From the slight increase in Shockley-Read-Hall recombination in each of the three devices, reduced local gain—optical mode overlap—may be seen to account for some of the decrease in efficiency. More important are the increases in the superlinear spontaneous and Auger recombination mechanisms, much more severe in the case of the device without current guides [Fig. 6(b)] than of those with [Fig. 6(a) and (c)].

The overriding impression from Fig. 6, however, is that leakage through parasitic paths overwhelms any of the preceding effects and is primarily responsible for the efficiency roll-off seen at different points on the L - I characteristics of the three devices. The larger voltage required to inject a given current into the active region of the device without current

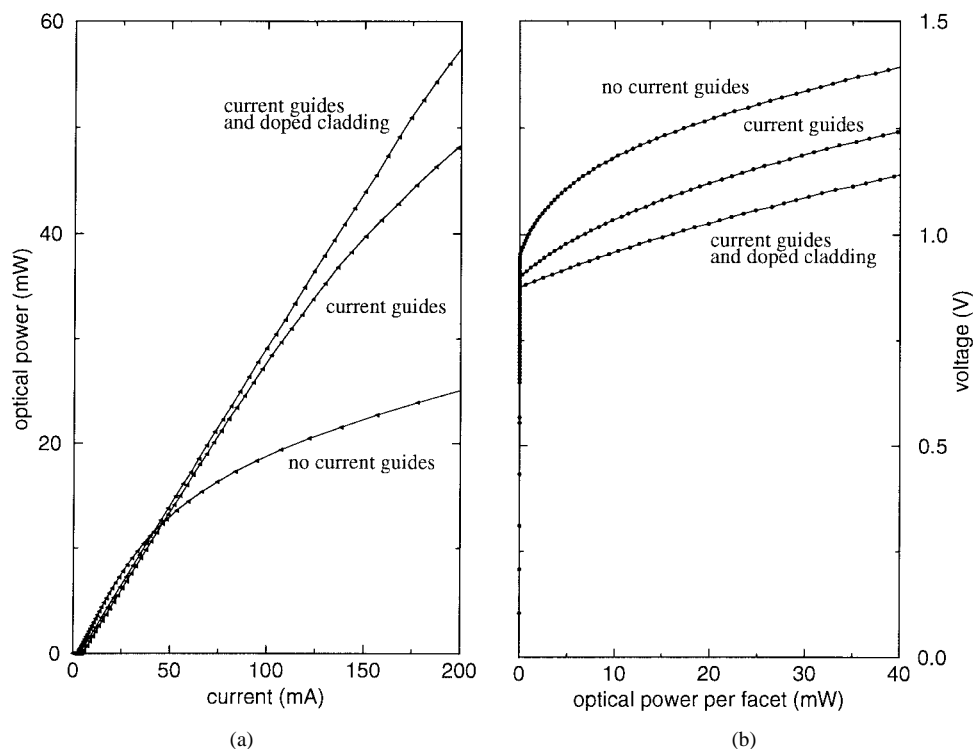


Fig. 4. Simulation: the effect of hybrid injection on the performance of an LCI laser.

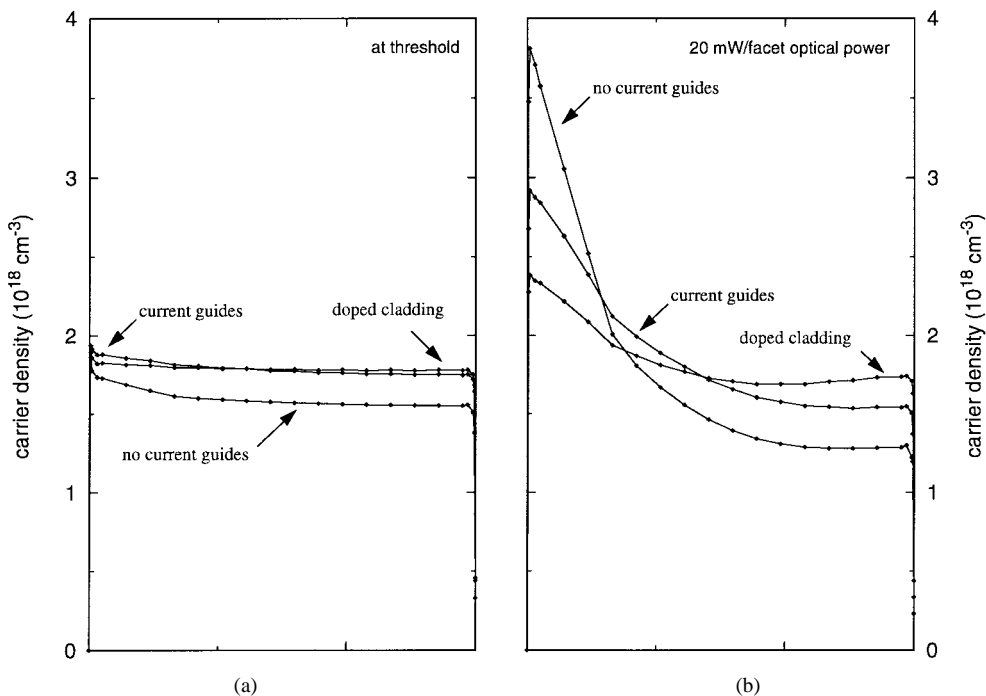


Fig. 5. Simulation: lateral carrier density profiles for the devices of Fig. 3, considered at (a) threshold and (b) 20-mW/facet optical power.

guides is accompanied by increased leakage through parallel parasitic paths which see this same larger voltage difference.

It is at this point worth considering the origins of series resistance in a lateral current injection laser in order to find other ways in which to reduce its importance and enable high-power low-leakage operation. It was recently shown [12] that above the lasing threshold by far the largest component of the differ-

ential series resistance above threshold in a typical LCI laser comes from the increase in voltage applied across heterojunction between the p-type contact and the active region in order to inject more current into the active region. (This phenomenon and its implications have also been studied in the vertical injection case [17]). The voltage drop across the P-i heterojunction increases approximately as the logarithm of the current density

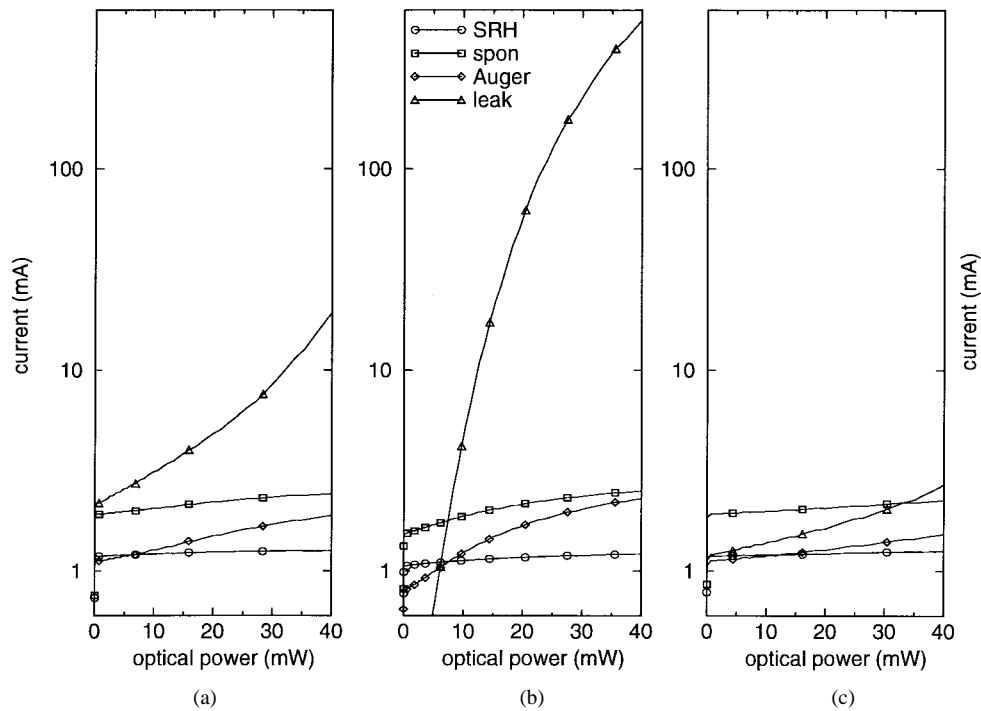


Fig. 6. Simulation: current components as a function of output optical power per facet for the laser structures illustrated in Fig. 3: (a) current guides, (b) no current guides, and (c) doped cladding.

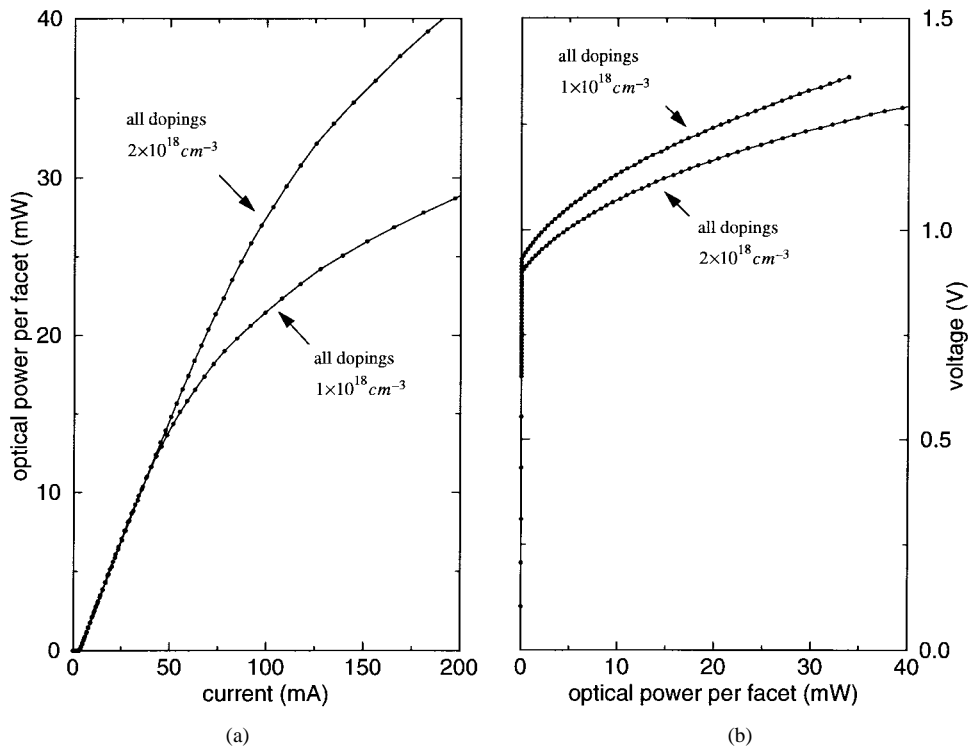


Fig. 7. Simulation: comparison of identical structures (both employing current guides) with different doping levels.

and decreases as $\ln(\mu_p N_A)$ (where μ_p is the hole mobility and N_A the contact acceptor concentration). The proportionality $V_{\text{heterojunction}} \sim \ln(J)$ can be used to account for the role of current guides in lowering series resistance: for a given total current injected into the active region, current guides reduce the average current density by increasing the injection area.

We studied the effect of p-contact doping on series resistance and leakage effects simulating a device identical to

that of Fig. 3(b) but with all dopings reduced from $2 \times 10^{18} \text{ cm}^{-3}$ to $1 \times 10^{18} \text{ cm}^{-3}$. The resulting $L-I$ and $V-L$ (Fig. 7) reveal that this moderate reduction in doping leads to a much earlier roll-off in the $L-I$ characteristic. LCI laser performance is a sensitive function of p-contact doping in the range of technological feasibility.

While the resistance of the heterojunction between the high-bandgap p-contact and the active region is determined by the

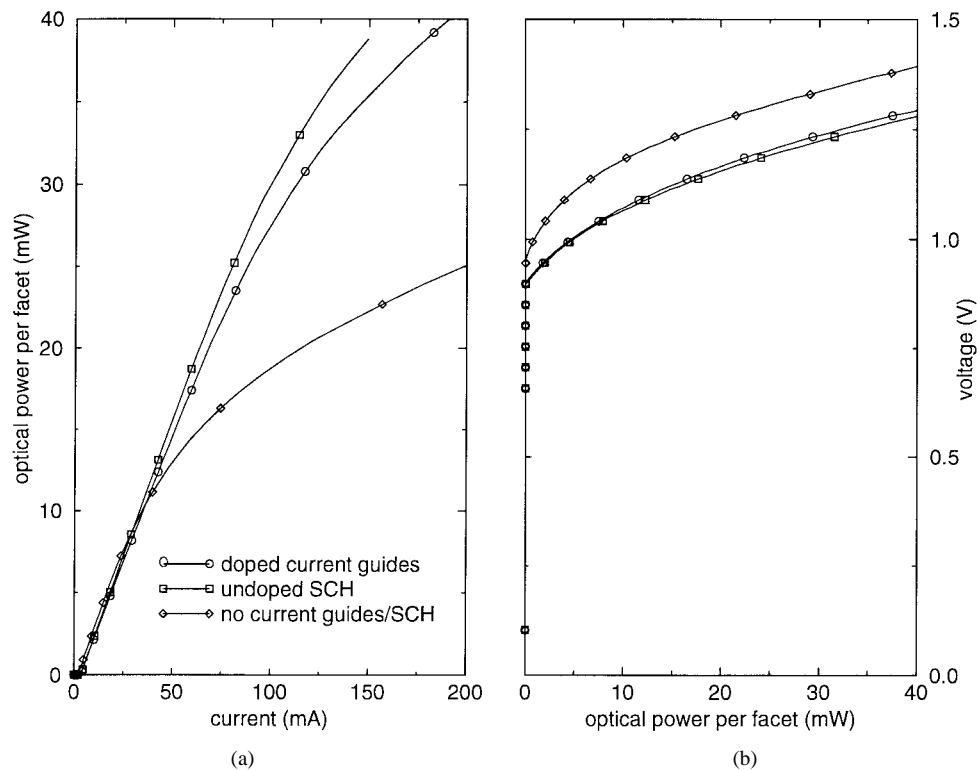


Fig. 8. Performance of LCI lasers with doped versus undoped current guides (device with no current guides at all also shown as reference).

doping of the p-contact, an SCH region with intermediate composition and no intentional doping could exhibit ambipolar conduction at moderate biases and consequent hybrid injection. This undoped layer could therefore serve to lower the series resistance of the active region. In order to test this hypothesis, we compared the performance of another set of three structures: one with doped current guides ($\lambda = 1.3 \mu\text{m}$), one with no current guides, and one with an *undoped* SCH region ($\lambda = 1.3 \mu\text{m}$). All doped regions were doped to a level of $2 \times 10^{18} \text{ cm}^{-3}$. The result L - I and V - I characteristics, shown in Fig. 8, indicate that the device with an undoped SCH in fact performs *better* than that with doped current guides, and much better than the device without current guides. At the lasing threshold, an appreciable population of electrons and holes co-exist in the SCH and contribute to a moderate ambipolar conductance. The reason for the somewhat superior performance of the undoped current guides over the doped current guides is that both guides, top and bottom, participate in *hole* injection in the undoped case. Since the dominant series resistance term to be reduced is associated with hole injection, the above-threshold differential resistance of the active region is best reduced by maximizing the area available for hole injections.

IV. IMPLICATIONS FOR LCI LASER DESIGN

The preceding results point to a number of conclusions relevant to the design of improved LCI lasers. We have found that a nonuniformity in the lateral carrier density may not, on its own, be a source of severe degradation in LCI laser output. It is a related phenomenon—the high series resistance of LCI laser active region—which had a more important impact on device performance in all of the cases considered herein.

We have not demonstrated the importance of reducing the *total* series resistance from contact to contact—undoubtedly important if Joule heating is taken into account—but only the resistance across the active region itself.

We may envision a number of ways which could potentially be employed in concert in order to postpone the onset of LCI laser efficiency roll-off.

- 1) Increase the aspect ratio of active region thickness to contact separation.
- 2) Maximize, to the degree made possible by technological limitations, the p-contact doping in order to minimize the differential resistance of the p-contact to active region heterojunction. (This assumes that holes are the limiting carrier, i.e., $\mu_h \ll \mu_e$.)
- 3) Maximize the effective area of the injection path for a given current. Current guides—be they doped or undoped (and of a bandgap fairly close to that of the active region)—represent an effective means of reducing the average injected current density for a given injected current. There is of course a tradeoff to be found, since using very thick current guides could offset many of the benefits of lateral injection (e.g., reduced free-carrier absorption and associated wavelength chirp).
- 4) Increase the ambipolar mobility of the active region via the use of strain-compensated multi-quantum well structures.
- 5) Increase the resistance of the parasitic paths using a technique such as iron doping of the cladding material.
- 6) Decrease the thickness of *contacted* leakage paths by performing the minimum amount of regrowth required to contact the active region (including current guides) only.

Since a number of tools are available in reducing the differential resistance of the active region, it is worth developing a “rule of thumb” as to the differential resistance which one should aim for in a given application. The ratio of the current leaking through the parasitic path to that being injected into the active region is given very approximately by

$$\frac{I_{\text{leak}}}{I_{\text{active}}} \approx \frac{t_{\text{leak}}}{t_{\text{active}}} \exp \left\{ -\frac{[E_{g(\text{leak})} - E_{g(\text{active})}] - q\Delta V}{kT} \right\}$$

where $\Delta V = V - E_{g(\text{active})}$ is the “excess voltage” applied across the active region, t_{active} is the thickness of the active region and t_{leak} is the thickness of the leakage path which is contacted. If the development of the voltage above may be described approximately using a differential resistance R_D , then the ratio may be written

$$\frac{I_{\text{leak}}}{I_{\text{active}}} \approx \frac{t_{\text{leak}}}{t_{\text{active}}} \exp \left\{ -\frac{[E_{g(\text{leak})} - E_{g(\text{active})}]}{kT} \right\} \cdot \exp \left(\frac{qIR_d}{kT} \right).$$

For example, suppose it is desired to obtain an LCI laser producing 20 mW/facet of optical power at 1.55 μm and using InP as the contact material. In the best case, if the differential quantum efficiency were 100%, $I_{\text{th}} + 50$ mA of current would have to be injected into the active region in order to sustain 20-mW/facet output power. If the active region were 0.1 μm thick and the thickness of the contacted leakage path 2 μm , then at room temperature, in order for $I_{\text{leak}}/I_{\text{active}} < \frac{1}{10}$, we would require an active region differential resistance of less than 7 Ω . As seen in [12], this value is somewhat less than that which would be obtained if no special resistance-lowering measures were adopted.

V. CONCLUSIONS

We believe that the large active region differential resistance of many previous LCI lasers has been an important contributor to high leakage and disappointing performance. We have found that minor technological improvements (e.g., maximized contact doping) and structural modifications (e.g., current guides) may have major impacts on device performance in view of the exponential dependence of leakage current on differential resistance. These findings hold great promise for future generations of LCI lasers and motivate continued theoretical probing of the internal operating mechanisms of this promising class of devices.

REFERENCES

- [1] E. H. Sargent, G. L. Tan, and J. M. Xu, “Physical model of OEIC-compatible lateral current injection lasers,” *IEEE J. Select. Topics Quantum Electron.*, vol. 3, pp. 507–512, 1997.
- [2] Y. Kan, M. Yamanishi, M. Okuda, K. Mukaiyama, T. Ohnishi, M. Kawamoto, and I. Suemune, “Quantum-confined field-effect light emitters with high-speed switching capability,” *Appl. Phys. Lett.*, vol. 55, pp. 1149–1151, 1989.
- [3] I. Suemune, T. Takeoka, M. Yamanishi, and Y. Lee, “Gain-switching characteristics and fast transient of three-terminal size-effect modulation laser,” *IEEE J. Quantum Electron.*, vol. QE-22, pp. 1900–1908, 1986.

- [4] A. Furuya, M. Makiuchi, O. Wada, and T. Fujii, “AlGaAs/GaAs lateral current injection multiquantum well (LCI-MQW) laser using impurity-induced disordering,” *IEEE J. Quantum Electron.*, vol. 24, pp. 2448–2453, 1988.
- [5] Y. Honda, I. Suemune, N. Yauhira, and M. Yamanishi, “Continuous-wave operation of a lateral current injection ridge waveguide AlGaAs/GaAs laser with a selectively-doped heterostructure,” *Jpn. J. Appl. Phys.*, vol. 30, pp. 990–991, 1991.
- [6] J. Ohta, K. Kuroda, K. Mitsunaga, K. Kyuma, K. Hamanaka, and T. Nakayama, “Buried transverse-junction stripe laser for optoelectronic-integrated circuits,” *J. Appl. Phys.*, vol. 61, pp. 4933–4935, 1987.
- [7] Y. Kawamura, Y. Noguchi, and H. Iwamura, “Lateral current injection InGaAs/InAlAs MQW lasers grown by GSMBE/LPE hybrid method,” *Electron. Lett.*, vol. 29, pp. 102–104, 1993.
- [8] Y. Suzuki, S. Mukai, H. Yajima, and T. Sato, “Transverse junction buried heterostructure (TJ-BH) AlGaAs diode laser,” *Electron. Lett.*, vol. 23, pp. 384–385, 1987.
- [9] K. Oe, Y. Noguchi, and C. Caneau, “GaInAsP lateral current injection lasers on semi-insulating substrates,” *IEEE Photon. Technol. Lett.*, vol. 6, pp. 479–481, 1994.
- [10] D. A. Suda, H. Lu, T. Makino, and J. M. Xu, “An investigation of lateral current injection laser internal operation mechanisms,” *IEEE Photon. Technol. Lett.*, vol. 7, pp. 1122–1124, 1995.
- [11] E. H. Sargent, G. Tan, and J. M. Xu, “Lateral current injection lasers: Underlying mechanisms and design for improved high-power efficiency,” *J. Lightwave Technol.*, submitted for publication.
- [12] P. Rees, P. Blood, M. J. H. Vanhomerig, G. J. Davies, and P. J. Skevington, “The temperature dependence of threshold current of chemical beam epitaxy grown InGaAs/InP lasers,” *Appl. Phys. Lett.*, vol. 78, pp. 1804–1807, 1995.
- [13] P. Bhattacharya, Ed., *Properties of Lattice-Matched and Strained Indium Gallium Arsenide*. London, U.K.: INSPEC, 1993.
- [14] D. N. Nasledov, Y. G. Popov, N. V. Siukaev, and S. P. Starosel'tseva, *Sov. Phys. Semicond.*, vol. 3, p. 387, 1969.
- [15] G. L. Tan, N. Bewtra, K. Lee, and J. M. Xu, “A two-dimensional non-isothermal finite element simulation of laser diodes,” *IEEE J. Quantum Electron.*, vol. 29, pp. 822–835, 1993.
- [16] R. F. Kazarinov and M. R. Pinto, “Carrier transport in laser heterostructures,” *IEEE J. Quantum Electron.*, vol. 30, pp. 49–53, 1994.

Edward H. Sargent (S'97), for photograph and biography, see p. 365 of the February 1998 issue of this JOURNAL.

Kunishige Oe (M'87) was born in Kyoto, Japan, in 1948. He received the B.S., M.S., and Ph.D. degrees from Kyoto University, Kyoto, Japan, in 1971, 1973, and 1982, respectively.

In 1973, he joined NTT Electrical Communication Laboratories, where he worked on LPE growth and laser fabrication of GaInAsP–InP double heterostructures, which resulted in the first oscillation of 1.3- μm CW laser diodes in 1977. He moved to electronic device research in 1983 in which he researched fabrication and characterization of heterostructures with two-dimensional gases and developed heterostructure FET's. Since 1986, he has been working on advanced semiconductor lasers and semiconductor integrated optical circuits. He spent one year (1990–1991) at Bell Communication Research, Red Bank, NJ, as a Visiting Scientist. Recently, he left NTT to be a Professor at Kyoto Institute of Technology, Kyoto, Japan.

Dr. Oe is a member of the Japan Society of Applied Physics and the Institute of Electronics, Information and Communication Engineers of Japan.

Catherine Caneau, photograph and biography not available at the time of publication.

J. M. Xu (M'87–SM'91), for photograph and biography, see p. 365 of the February 1998 issue of this JOURNAL.